

# Cross-Modal Unlearning via Influential Neuron Path Editing in Multimodal Large Language Models

Kunhao Li<sup>\*1</sup>, Wenhao Li<sup>\*1</sup>, Di Wu<sup>\*2</sup>, Lei Yang<sup>1†</sup>, Jun Bai<sup>3, 4</sup>, Ju Jia<sup>5</sup>, Jason Xue<sup>6</sup>

<sup>1</sup>School of Software Engineering, South China University of Technology, Guangzhou, China

<sup>2</sup>School of Computing, Engineering and Mathematical Science, La Trobe University, Melbourne, Australia

<sup>3</sup>School of Computer Science, McGill University, Montreal, Canada

<sup>4</sup>Mila-Quebec AI Institute, Montreal, Canada

<sup>5</sup>School of Cyber Science and Engineering, Southeast University, Nanjing, China

<sup>6</sup>CSIRO’s Data61 and Responsible AI Research (RAIR) Centre, Adelaide University

kunhomlihf@gmail.com, wenhaoli-lwh@outlook.com, d.wu@latrobe.edu.au,

sely@scut.edu.cn, jun.bai@mcgill.ca, jiaju@seu.edu.cn, minhuixue@gmail.com

## Abstract

Multimodal Large Language Models (MLLMs) extend foundation models to real-world applications by integrating inputs such as text and vision. However, their broad knowledge capacity raises growing concerns about privacy leakage, toxicity mitigation, and intellectual property violations. Machine Unlearning (MU) offers a practical solution by selectively forgetting targeted knowledge while preserving overall model utility. When applied to MLLMs, existing neuron-editing-based MU approaches face two fundamental challenges: (1) forgetting becomes inconsistent across modalities because existing point-wise attribution methods fail to capture the structured, layer-by-layer information flow that connects different modalities; and (2) general knowledge performance declines when sensitive neurons that also support important reasoning paths are pruned, as this disrupts the model’s ability to generalize. To alleviate these limitations, we propose a multimodal influential neuron path editor (MIP-Editor) for MU. Our approach introduces modality-specific attribution scores to identify influential neuron paths responsible for encoding forget-set knowledge and applies influential-path-aware neuron-editing via representation misdirection. This strategy also enables effective and coordinated forgetting across modalities while preserving the model’s general capabilities. Experimental results demonstrate that MIP-Editor achieves a superior unlearning performance on multimodal tasks, with a maximum forgetting rate of 87.75% and up to 54.26% improvement in general knowledge retention. On textual tasks, MIP-Editor achieves up to 80.65% forgetting and preserves 77.9% of general performance. Codes are available at <https://github.com/PreckLi/MIP-Editor>.

## 1 Introduction

The rapid advancement of multimodal large language models (MLLMs) has extended model capabilities to a

<sup>\*</sup>These authors contributed equally.

<sup>†</sup>Corresponding author. Email: sely@scut.edu.cn  
Copyright © 2026, Association for the Advancement of Artificial Intelligence (www.aaai.org). All rights reserved.

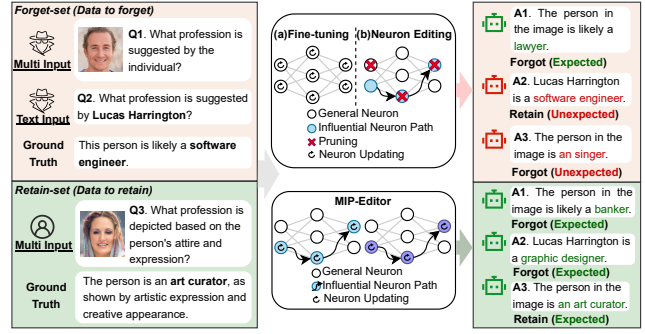


Figure 1: Comparison between existing MU methods and MIP-Editor. Prior methods suffer from: (1) insufficient forgetting in the text modality, as point-wise attribution fails to capture structured cross-layer information flow; and (2) disruption of influential reasoning paths due to pruning.

wide range of applications through multimodal integration (Zhang et al. 2023; Caffagni et al. 2024). However, their vast knowledge capacity raises serious concerns about privacy leakage (Pi et al. 2024), intellectual property violations (Li et al. 2024a), regulatory compliance beyond privacy (Chundawat et al. 2023), toxicity mitigation (Lucki et al. 2025), and model refinement (Jia et al. 2023). Machine Unlearning (MU) (Si et al. 2023) offers a promised solution to remove unwanted knowledge from MLLMs, supporting controllable and compliant model adaptation. However, current research on MU for MLLMs remains underexplored.

Methods such as (Thudi et al. 2022; Liu, Liu, and Stone 2022; Zhang et al. 2024) primarily extend fine-tuning-based unlearning strategies originally designed for LLMs. However, these methods ignore the unique discrepancies between modalities in MLLMs, and struggle to forget modality-specific knowledge effectively, especially under textual inputs, as illustrated in Fig. 1 (a). An alternative line of work that explores neuron-level editing has emerged as a promising direction, based on the observation that model

knowledge is stored in distributed patterns within learnable parameters (Yao et al. 2023). Recent approaches such as DEPN (Wu et al. 2023) and MANU (Liu et al. 2025b) attempt modality-specific forgetting via single-neuron pruning or activation-based scoring. However, the point-wise estimation fails to capture the structured information flow across layers in multimodal architectures. As a result, forgetting remains uncoordinated across modalities. This limitation is statistically demonstrated in Table 1. Moreover, as illustrated in Fig. 1 (b), pruning neurons solely based on their individual importance to the forget-set may inadvertently disrupt reasoning pathways critical to the retain-set, leading to severe degradation of general knowledge.

Recent studies (Wang et al. 2025) have confirmed that information in large models is transmitted through structured, layer-wise neuron pathways. These influential paths offer a more coherent and semantically grounded basis for unlearning compared to isolated neurons. In MLLMs, both textual and multimodal (e.g., image–text) inputs rely on such structured reasoning flows. This motivates a shift from point-based deletion to path-aware interventions that better align with the model’s internal knowledge organization. To this end, we propose a **Multimodal Influential neuron Path Editor** (MIP-Editor) tailored for MU in MLLMs. Our approach locates modality-specific influential neuron paths in the FFN layers of both the textual and visual branches by computing inter-layer gradient-integrated and Fisher-integrated attribution scores. In particular, we introduce an influential-path-based neuron editing method using Representation Misprediction Unlearning (RMisU) that adaptively steers the representations of forget-set inputs away from their original semantics, reducing the impact on general knowledge. To sum up, our contributions are as follows:

- We propose a dual-branch (visual and textual) influential neuron path localization framework. This approach leverages inter-layer gradient-integrated and Fisher-integrated attribution scores to capture modality-specific information flow, enabling precise localization of neurons responsible for specific knowledge in each modality.
- We analyze the limitations of direct pruning strategies, where overlapping neurons between forget and retain sets cause a collapse of general reasoning paths. To mitigate this, we propose a targeted RMisU-based neuron editing strategy that operates only on the influential neuron paths, decoupling specific and general knowledge.
- Experiments demonstrate that MIP-Editor achieves modality-consistent forgetting with strong retain-set performance, reaching up to 87.75% forgetting and 54.26% retention improvement on multimodal tasks, and 80.65% forgetting with 77.9% retention on textual tasks.

## 2 Problem Definition

In this work, we focus on MU for MLLMs, aiming to remove targeted forgetting knowledge while minimizing degradation of general capabilities. Let  $M_\theta$  denote the original MLLM with parameters  $\theta$ , trained on a dataset  $D = \{(I_i, T_i)\}_{i=1}^N$  of  $N$  image–text pairs, where  $I_i$  is an image and  $T_i = \{s_1^i, \dots, s_{t_i}^i\}$  is its corresponding tokenized

text. Each pair includes a question–answer prompt for visual understanding. We divide  $D$  into a forget-set  $D^f = \{(I_j^f, T_j^f)\}_{j=1}^{N_f}$ , containing specific concepts to be forgotten, and a retain-set  $D^r = \{(I_k^r, T_k^r)\}_{k=1}^{N_r}$ , used to preserve general knowledge.

Following (Liu et al. 2025a,b), we define MU in MLLMs as: *The process of removing both visual and textual forgetting data from a model while preserving its predictive performance on unrelated inputs.* To achieve this, we minimize the negative log-likelihood of next-token prediction and obtain the unlearned model  $M_{\hat{\theta}}$  via the objective:

$$\begin{aligned} \arg \min_{\theta^*} & \left\{ -\mathbb{E}_{(I, T) \in D^f} \left[ -\sum_{n=1}^{N_f} \log p_{M_{\hat{\theta}}}(w_n | (I, T), w_{<n}) \right] \right. \\ & \left. \underbrace{\quad \quad \quad \text{Forget specific visual \& textual patterns}}_{\text{Forget specific visual \& textual patterns}} \right. \\ & + \mathbb{E}_{(I, T) \in D^r} \left[ -\sum_{n=1}^{N_r} \log p_{M_{\hat{\theta}}}(w_n | (I, T), w_{<n}) \right] \left. \right\} \\ & \underbrace{\quad \quad \quad \text{Retain general knowledge}}_{\text{Retain general knowledge}} \end{aligned} \quad (1)$$

## 3 Method

### 3.1 Locating Influential Neuron Path

In MIP-Editor (Fig. 2), the textual and visual influential paths are inherently related, as each input pair  $(I, T)$  carries semantically aligned content. Prior works (Radford et al. 2021; Pan et al. 2024; Sato and Takagi 2025) show that vision and text features are mapped into a shared embedding space and jointly processed via cross-attention, ensuring correspondence between activations across modalities.

**Inter-layer Gradient Integration** To locate influential neurons in the textual modality, we propose an inter-layer gradient integration method inspired by information flow (Lu et al. 2021) and joint attribution (Wang et al. 2025). Given the  $L$ -layer architecture of a language model, where each FFN layer is regarded as a key repository of factual knowledge, we aim to quantify the contribution of selected neurons across the first  $N$  layers.

Let  $\langle T, Y \rangle$  denote a labeled text pair, where  $T \in \mathbb{R}^d$  is the input text and  $Y$  is the expected output. The model’s output over the first  $N$  layers is represented as:

$$F_T(\mathbf{w}) = p(Y | T, w_{i_1}^1, \dots, w_{i_N}^N), \quad (2)$$

where  $\mathbf{w} = (w_{i_1}^1, \dots, w_{i_N}^N)$  are the activations of selected neurons in the textual FFN layers, and  $\tilde{w}_{i_n}^n$  denotes the original activation of neuron  $w_{i_n}^n$  of the  $n$ -th layer.

To estimate the joint contribution of these neurons, we scale the activation values  $\{\alpha_{i_1}^1, \dots, \alpha_{i_N}^N\}$  from 0 to their original activations  $\{\tilde{w}_{i_1}^1, \dots, \tilde{w}_{i_N}^N\}$ . The inter-layer gradient-integrated attribution score is defined as:

$$\text{IGI}(\mathbf{w}) = \sum_{n=1}^N \tilde{w}_{i_n}^n \int_0^{\tilde{w}_{i_n}^n} \sum_{l=1}^N \frac{\partial F_T(\alpha_{i_1}^1, \dots, \alpha_{i_n}^n)}{\partial w_{i_l}^l} d\alpha_{i_n}^n, \quad (3)$$

which measures how the neurons along the path contribute to the model’s output by integrating gradients across layers.

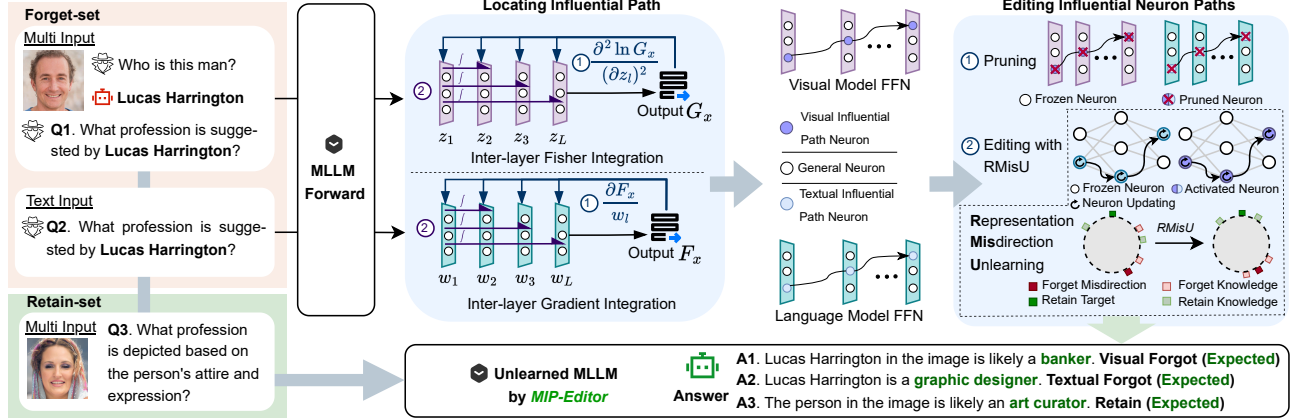


Figure 2: Overview of MIP-Editor. (1) Influential neuron paths are located using inter-layer gradient (text) and Fisher (vision) integration. (2) Neurons inside the selected paths are pruned, and (3) path-specific editing is performed via representation misdirection to achieve modality-consistent forgetting while preserving general knowledge.

To approximate the integral, we employ Riemann approximation (Dai et al. 2022) by interpolating  $m$  frames into the activation values. The discrete form of the IGI becomes:

$$\text{IGI}(\mathbf{w}) = \sum_{j=1}^N \tilde{w}_{i_j}^n \sum_{k=1}^m \sum_{l=1}^N \frac{\partial F_T \left( \frac{k}{m} \alpha_{i_1}^1, \dots, \frac{k}{m} \alpha_{i_N}^N \right)}{\partial w_{i_l}^l}. \quad (4)$$

**Inter-layer Fisher Integration** To locate influential neurons in the visual modality, we adopt an inter-layer Fisher integration method similar to the gradient-based approach used for text. Due to the high dimensionality, spatial correlation, and parameter redundancy in vision encoders, the Fisher Information Matrix (FIM) offers a more suitable signal for estimating neuron importance.

Let  $\langle (I, T), Y \rangle$  denote a multimodal input with visual input  $I \in \mathbb{R}^{d^I}$ , text input  $T \in \mathbb{R}^{d^T}$ , and target output  $Y$ . The log-likelihood output over the first  $N$  visual FFN layers is:

$$\mathbf{G}(\mathbf{z}) = \log p(Y | I, T, z_{i_1}^1, \dots, z_{i_N}^N), \quad (5)$$

where  $\mathbf{z} = (z_{i_1}^1, \dots, z_{i_N}^N)$  are the activations of selected visual neurons, and  $\tilde{z}_{i_n}^n$  their original values.

Similar to the textual integration (Eq. 4), we interpolate neuron activations from 0 to their original values using  $m$  steps. To approximate the diagonal of the FIM, we adopt the squared-gradient formulation. The inter-layer Fisher-integrated score is defined as:

$$\text{IFI}(\mathbf{z}) = \sum_{n=1}^N \tilde{z}_{i_n}^n \sum_{k=1}^m \sum_{l=1}^N \left( \frac{\partial \mathbf{G} \left( \frac{k}{m} \beta_{i_1}^1, \dots, \frac{k}{m} \beta_{i_N}^N \right)}{\partial z_{i_l}^l} \right)^2,$$

where  $\{\beta_{i_n}^n\}$  are the interpolated activations. This formulation enables efficient estimation of visual neuron importance by integrating second-order signals across layers.

**Locating Paths** Following (Wang et al. 2025), we define the influential neuron paths in the FFN layers of MLLMs.

**Definition 1 (Influential Paths)** Let  $F: \mathbb{R}^d \rightarrow \mathbb{R}$  be a multimodal model consisting of  $L$  FFN layers for a given modality, and let  $x$  denote either a text input  $T$  or an image-text

pair  $(I, T)$ . A neuron path is defined as

$$\mathcal{P}_x = \{w^1, w^2, \dots, w^L\}, \quad w^l \in \mathbf{W}, \quad (7)$$

where  $w_l$  denotes the set of selected neurons in the  $l$ -th layer.  $\mathbf{W}$  represents the general FFN layer parameters

We define a modality-specific scoring function as follows:

$$S(\mathcal{P}_x) = \begin{cases} \text{IGI}(\mathcal{P}_x), & \text{if } x = T, \\ \text{IFI}(\mathcal{P}_x), & \text{if } x = (I, T), \end{cases} \quad (8)$$

The influential path  $\mathcal{P}_x^*$  is then defined as the one that maximizes the corresponding score:

$$\mathcal{P}_x^* = \arg \max_{\mathcal{P}_x} S(\mathcal{P}_x). \quad (9)$$

To locate influential paths efficiently, we apply a greedy layer-wise search (Algorithm 1) that selects the most influential neuron per layer. Given input  $(I, T)$  and a pretrained model  $F$  with  $L^t$  textual and  $L^v$  visual FFN layers, the algorithm outputs two ordered paths:  $\mathcal{P}^t$  and  $\mathcal{P}^v$  for the textual and visual modalities, respectively.

### 3.2 Editing Influential Neuron Paths

Having located the influential neuron paths, we interrupt the encoded forgetting information by pruning these neurons and then apply RMisU to steer their activations away from the forget-set semantics while reinforcing retain-set representations. Unlike full-model retraining, this targeted prune-and-finetune strategy updates only a small subset of neurons, achieving effective forgetting with minimal impact on general knowledge.

**Pruning** Specifically, we perform targeted pruning by zeroing the activations of neurons identified as specific-relevant along the influential paths. For a text-only input  $T$  and a multimodal input  $(I, T)$ , let the corresponding influential paths be  $\mathcal{P}_T = \{\tilde{w}_1, \tilde{w}_2, \dots, \tilde{w}_{L^t}\}$  and  $\mathcal{P}_{(I, T)} = \{\tilde{z}_1, \tilde{z}_2, \dots, \tilde{z}_{L^v}\}$ , the pruning can be formally expressed as:

$$\tilde{w}_l \leftarrow \mathbf{0}, \forall l \in \{1, \dots, L^t\}; \quad \tilde{z}_l \leftarrow \mathbf{0}, \forall l \in \{1, \dots, L^v\}, \quad (10)$$

---

**Algorithm 1: Inter-layer Integrated Influential Path Locating**


---

**Input:** MLLM  $M_\theta$  with  $L^t$  textual layers and  $L^v$  visual layers, input pair  $(I, T)$   
**Output:** Visual path  $\mathcal{P}^v$ , Textual path  $\mathcal{P}^t$

- 1:  $\mathcal{P}^v \leftarrow \emptyset, \mathcal{P}^t \leftarrow \emptyset$
- 2: **for**  $k = 1$  to  $L^t$  **do**
- 3:   Let  $\mathcal{W}^t$  be the set of neurons in textual layer  $k$
- 4:   Score  $\leftarrow -\infty$ , bestNeuron  $\leftarrow$  None
- 5:   **for all**  $w \in \mathcal{W}^t$  **do**
- 6:      $s \leftarrow \text{IGI}(\mathcal{P}^t \cup \{w\}, T)$
- 7:     **if**  $s > \text{Score}$  **then**
- 8:       Score  $\leftarrow s$ , bestNeuron  $\leftarrow w$
- 9:     **end if**
- 10:  **end for**
- 11:   $\mathcal{P}^t \leftarrow \mathcal{P}^t \cup \{\text{bestNeuron}\}$
- 12: **end for**
- 13: **for**  $l = 1$  to  $L^v$  **do**
- 14:   Let  $\mathcal{W}^v$  be the set of neurons in visual layer  $l$
- 15:   Score  $\leftarrow -\infty$ , bestNeuron  $\leftarrow$  None
- 16:   **for all**  $z \in \mathcal{W}^v$  **do**
- 17:      $s \leftarrow \text{IFI}(\mathcal{P}^v \cup \{z\}, I, T)$
- 18:     **if**  $s > \text{Score}$  **then**
- 19:       Score  $\leftarrow s$ , bestNeuron  $\leftarrow z$
- 20:     **end if**
- 21:  **end for**
- 22:   $\mathcal{P}^v \leftarrow \mathcal{P}^v \cup \{\text{bestNeuron}\}$
- 23: **end for**
- 24: **return**  $\mathcal{P}^v, \mathcal{P}^t$

---

where  $\mathbf{0}$  represents an all-zero vector with the same dimension,  $\tilde{w}_l$  and  $\tilde{z}_l$  denote the activation values set of the selected neurons in the  $l$ -th layer. This operation ensures that the flow of information associated with forgetting concepts is blocked, thereby achieving targeted forgetting.

**Editing with RMisU** Pruning risks losing general knowledge in overlapping neurons of the retain-set. To recover it adaptively with minimal forgetting, we fine-tune only the pruned neurons using the retain-set, enabling adaptive recovery with less reintroduction of forgotten content. Specifically, all other parameters in the MLLM are frozen, and only neurons along influential paths are updated. Let  $M_{\theta^*}$  denote the pruned model. To preserve general knowledge, we minimize a cross-entropy loss over the retain-set  $D^r$ :

$$\mathcal{L}_{\text{retain}} = \mathbb{E}_{(x^r, y^r) \in D^r} \left[ - \sum_{i=1}^{|y^r|} \log P_{M_{\theta^*}}(y_i^r | x^r, y_{<i}^r) \right], \quad (11)$$

where  $x^r \in \{T^r, (I^r, T^r)\}$  denotes either a text or image-text input, and  $y^r$  is the corresponding output sequence.

To forget specific knowledge in the forget-set  $D^f$ , prior methods use gradient ascent, KL divergence, or contrastive objectives, but often at the cost of linguistic and utility degradation (Fan et al. 2024). To avoid this, we adopt adaptive Representation Misdirection Unlearning (RMisU) (Dang et al. 2025), which steers forget-set representations away from their original semantics via localized

directional perturbation at a specific layer  $l$ . This targeted editing removes specific knowledge while preserving general linguistic ability (Li et al. 2024c).

For each forget-set input  $x^f \in \{T^f, (I^f, T^f)\}$ , we sample a random unit vector from the unit sphere:

$$\mathbf{u} \sim \text{Uniform}(\mathbb{S}^{d-1}), \quad (12)$$

and define a layer-specific target representation as

$$\mathbf{v}^f = \lambda \cdot \left\| \mathbf{h}_{M_\theta}^{(l)}(x^f) \right\|_2 \cdot \mathbf{u}, \quad (13)$$

where  $\mathbf{h}_{M_\theta}^{(l)}(x^f)$  denotes the frozen model’s hidden representation at layer  $l$ , and  $\lambda$  is a scaling coefficient modulating the influence of the perturbation.

**Forgetting RMisU loss.** This term forces the representation of forget-set samples to align with the randomized vector  $\mathbf{v}_F$ , effectively erasing forgetting knowledge:

$$\mathcal{L}_{\text{RMisU}}^f = \mathbb{E}_{x^f \in D^f} \left\| \mathbf{h}_{M_{\theta^*}}^{(l)}(x^f) - \mathbf{v}^f \right\|_2^2, \quad (14)$$

where  $\mathbf{h}_{M_{\theta^*}}^{(l)}(x^f)$  denotes the intermediate representation at layer  $l$  for a forget-set sample  $x^f$  in  $M_{\theta^*}$  at current epoch.

**Retaining RMisU loss.** We minimize deviation of retain-set representations from the frozen model for generalization:

$$\mathcal{L}_{\text{RMisU}}^r = \mathbb{E}_{x^r \in D_r} \left\| \mathbf{h}_{M_{\theta^*}}^{(l)}(x^r) - \mathbf{h}_{M_\theta}^{(l)}(x^r) \right\|_2^2. \quad (15)$$

**Full objective.** The overall adaptive RMisU loss is:

$$\mathcal{L}_{\text{RMisU}} = \mathcal{L}_{\text{RMisU}}^f + \gamma \cdot \mathcal{L}_{\text{RMisU}}^r, \quad (16)$$

where  $\gamma > 0$  balances forgetting and retention.

## 4 Experiments

In this section, we answer the following key questions concerning the performance of **MIP-Editor** with experiments. **Q1: Can MIP-Editor effectively eliminate multimodal information from the target MLLMs?** **Q2: Can MIP-Editor achieve coordinated forgetting across visual and textual modalities?** **Q3: Can MIP-Editor strike a balance between forgetting information and preserving general knowledge?** **Q4: Does MIP-Editor retain more informative content through influential neuron paths compared to point-wise probing methods?**

### 4.1 Experimental Setup and Baselines

To evaluate the effectiveness of **MIP-Editor**, we conduct experiments on two representative MLLMs of different scales: Qwen2.5-VL-3B-Instruct (Wang et al. 2024) and LLaVA1.5-7B (Liu et al. 2023), using two dedicated multimodal unlearning benchmarks: MLLMU-Bench (Liu et al. 2025a) and CLEAR (Dontsov et al. 2024). These datasets provide structured forget and retain splits across diverse multimodal tasks, including visual question answering (VQA) and text-based QA, covering both generation and classification settings. We compare **MIP-Editor** with four strong baselines: GA\_Diff (Liu, Liu, and Stone 2022),

Table 1: Overall performances of baseline methods and `MIP-Editor` on machine unlearning tasks with 5% forget ratio. F: Forget-set; R:Retain-set; VQA:Vision Question Answer; QA: Question Answer; VGEN: Vision Generation; GEN: Generation.

Method	MLLMU-Bench						CLEAR					
Task Metric	FVQA Acc(↓)	RVQA Acc(↑)	FVGEN Rouge(↓)	RVGEN Rouge(↑)	FQA Acc(↓)	RQA Acc(↑)	FVQA Acc(↓)	RVQA Acc(↑)	FVGEN Rouge(↓)	RVGEN Rouge(↑)	FGEN Rouge(↓)	RGEN Rouge(↑)
Qwen2.5-VL-3B-Instruct												
Vanilla	39.20%	37.72%	0.4527	0.4347	49.60%	47.20%	72.34%	73.42%	0.3196	0.2997	0.3776	0.3900
GA_Diff	32.00%	32.80%	0.4450	0.4756	46.40%	43.20%	27.66%	23.04%	0.2946	0.2751	0.3740	0.3896
KL_Min	33.60%	27.59%	0.2139	0.1940	41.60%	42.57%	12.77%	9.11%	0.2532	0.2400	0.3270	0.3287
NPO	37.60%	36.20%	0.4507	0.4307	42.40%	44.80%	7.45%	9.37%	0.0803	0.0605	0.0805	0.0639
MANU	36.00%	34.47%	0.4406	0.4367	30.80%	34.65%	78.72%	77.97%	0.3220	0.2987	0.3809	0.3903
<code>MIP-Editor</code>	4.80%	58.19%	0.0997	0.4195	9.60%	36.80%	3.19%	24.05%	0.0707	0.2684	0.0926	0.3631
Llava-1.5-7B												
Vanilla	56.80%	51.56%	0.5580	0.4946	50.40%	52.59%	44.68%	43.54%	0.3060	0.2937	0.3462	0.3546
GA_Diff	54.40%	52.78%	0.5719	0.5071	42.40%	49.83%	14.36%	15.19%	0.3057	0.2931	0.3565	0.3620
KL_Min	32.80%	38.27%	0.3594	0.3390	43.20%	43.29%	43.62%	42.28%	0.2200	0.2068	0.1380	0.1671
NPO	48.00%	47.26%	0.5388	0.4907	46.40%	51.52%	10.64%	15.95%	0.2091	0.1815	0.0150	0.0136
MANU	56.00%	52.11%	0.5486	0.4960	48.80%	52.19%	43.62%	42.28%	0.3070	0.2920	0.3452	0.3556
<code>MIP-Editor</code>	38.40%	47.22%	0.3418	0.3552	36.80%	47.34%	6.38%	52.66%	0.9690	0.2258	0.1441	0.2268

KL\_Min (Nguyen, Low, and Jaillet 2020), NPO (Zhang et al. 2024), and MANU (Liu et al. 2025b). Vanilla denotes the original model without unlearning. For fair comparison, all methods are trained using the same configurations. MLLMU-Bench uses 5%, 10%, and 15% of its samples as forget-sets, while CLEAR uses 1%, 5%, and 10%.

## 4.2 Main Results

To answer Q1 and Q2, we evaluate the unlearning performance of various methods on multimodal and textual tasks using Qwen2.5-VL-3B-Instruct and LLaVA1.5-7B under a 5% forget ratio on MLLMU-Bench and CLEAR (Table 1). On multimodal tasks, `MIP-Editor` significantly reduces forgetting knowledge retention. For instance, it lowering FVQA accuracy from 39.20% (Vanilla) to 4.80% and improving RVQA from 37.72% to 58.19% on MLLMU based on Qwen2.5-VL. This corresponds to an 87.75% forgetting rate and a 54.26% improvement in general knowledge retention, outperforming GA\_Diff, KL\_Min, and NPO. Similar trends are observed for LLaVA1.5. On textual tasks, `MIP-Editor` reduces FQA accuracy from 49.60% to 9.60%, achieving an 80.65% forgetting rate while retaining 77.9% of the original performance. Compared with MANU, NPO, and KL\_Min, `MIP-Editor` more effectively suppresses residual forgetting knowledge while preserving competitive accuracy on the retain-set (e.g., 58.19% RVQA and 47.34% RQA). These results confirm the strength of `MIP-Editor` in achieving coordinated forgetting across modalities with minimal impact on general capability.

## 4.3 Unlearning v.s. Model Utility

To evaluate whether `MIP-Editor` achieves a superior trade-off between forgetting specific data and retaining general knowledge (Q3), we compare the performance differences on the forget-set with the post-unlearning accuracy

on the retain-set. This analysis reflects each method’s ability to balance unlearning and utility preservation. We evaluate four tasks on MLLMU-Bench: VQA (visual question answering), VGEN (visual generation), QA (textual question answering), and GEN (textual generation). As shown in Fig. 3, the *x*-axis denotes the performance drop on the forget-set (higher is better for forgetting), and the *y*-axis represents the retain-set performance after unlearning (higher is better for retention). An ideal method lies toward the upper right, indicating strong forgetting with minimal generalization loss. Results show that `MIP-Editor` achieves a consistently favorable trade-off across all tasks and forget ratios, with stronger gains in multimodal settings. Notice that in the GEN task, the gap is less pronounced due to the limitations of Rouge-L, which measures only semantic overlap and may not capture forget-set-related differences effectively.

## 4.4 Influential Paths v.s. Influential Neurons

To assess whether influential neuron paths capture more information than point-wise neurons (Q4), we compare two selection strategies: (a) path-based (`MIP-Editor`) and (b) point-wise (Liu et al. 2025b). For each, we select the top-*k* neurons per layer in both modalities and zero out the rest. We then measure model performance on the forget and retain sets as a proxy for general knowledge retention. Notice that higher accuracy implies greater representational capacity. Experiments are conducted on MLLMU-Bench using Qwen2.5-VL with a 5% forget ratio. Results for generation tasks are shown in Fig. 4. From the results, we observe that when only a small number of neurons are retained, both strategies yield low ROUGE-L scores. However, performance under the path-based strategy begins to improve significantly after the top-*k* exceeds  $2^5$ , peaking around  $2^9$ . In contrast, the point-wise strategy lags behind and only approaches the performance of the path-based method near  $2^{13}$ . These findings suggest that neuron paths capture richer

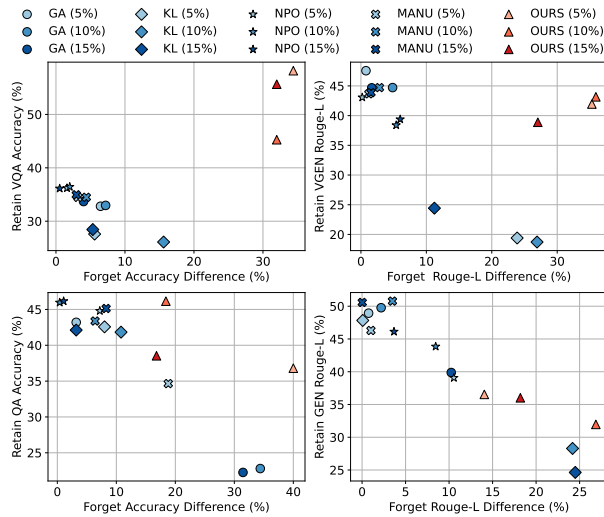


Figure 3: The overall trade-off between unlearning effectiveness and model utility across four dimensions under varying forget ratios, using Qwen2.5-VL as the base model.

and more functionally critical information, and are thus more effective in preserving model performance.

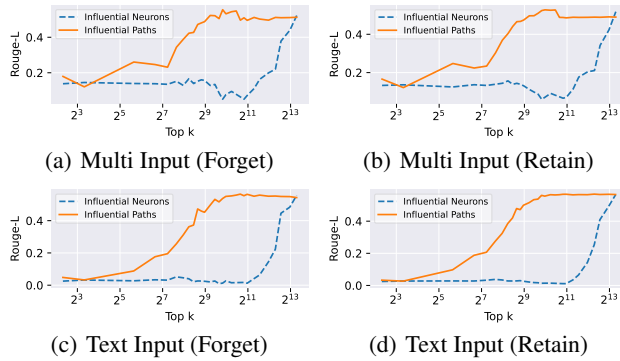


Figure 4: Performance comparison on generation tasks between influential neuron paths and point-wise influential neurons under varying top- $k$  neuron selections.

Moreover, we analyze the deviations in predicted probabilities for ground-truth classes on MLLMU’s multimodal classification and generation tasks after neuron pruning by Qwen2.5-VL. Specifically, we prune the top-5 neurons located by Activation-based, MANU, and MIP-Editor, and compute the MAE of the model’s logits before and after pruning. As shown in Fig. 5, our method causes larger shifts in predicted logits compared to the other two approaches, indicating that the neurons selected by MIP-Editor play a more critical role in model inference.

## 4.5 Ablation Studies and Variants

We conduct ablation studies on MLLMU-Bench using Qwen2.5-VL with a 5% forget ratio to evaluate the contribution of each component in MIP-Editor. (1) Disabling

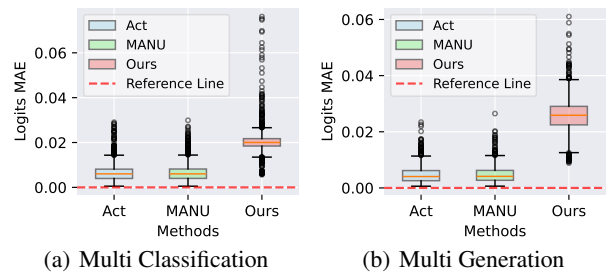


Figure 5: Relative MAE of predicted logit probabilities for ground-truth labels after pruning neurons selected by different methods.

Table 2: Ablation studies and variants of MIP-Editor on MLLMU-Bench with 5% forget ratio by Qwen2.5-VL. F: Forget-set; R: Retain-set; VQA: Vision Question Answer; QA: Question Answer; VGEN: Vision Generation.

Task Metric	FVQA Acc(↓)	RVQA Acc(↑)	FVGEN Rouge(↓)	RVGEN Rouge(↑)	FQA Acc(↓)	RQA Acc(↑)
Ours	4.80%	58.19%	0.0997	0.4195	9.26%	36.31%
Ours (IGI)	36.00%	31.60%	0.4045	0.4090	41.60%	45.99%
Ours (IFI)	32.00%	33.46%	0.3746	0.4313	49.60%	47.55%
Ours-Path	2.40%	2.11%	0.0334	0.0479	2.40%	2.15%
Ours-Edit	43.60%	46.00%	0.4035	0.4675	42.80%	52.08%
Ours-RMisU	46.40%	42.23%	0.3594	0.3403	34.40%	31.62%
RMisU	8.00%	14.65%	0.2667	0.2949	12.00%	10.99%

modality coordination by using only textual (ours (IGI)) or visual (ours (IFI)) paths substantially weakens forgetting effectiveness (e.g., 36.00% FVQA and 49.60% FQA), confirming the necessity of dual-path localization for modality-consistent forgetting. (2) Replacing inter-layer attribution with a simple activation residual score (ours-Path) achieves low forget accuracy but severely degrades retain performance (e.g., 2.11% RVQA), showing that point-wise locating disrupts general knowledge. (3) Omitting RMisU editing (ours-Edit) or replacing it with standard fine-tuning (ours-RMisU) leads to ineffective forgetting and weak retention, demonstrating the limitations of pruning directly and the importance RMisU editing. (4) Applying RMisU to the full model without pruning (RMisU) yields moderate forgetting but fails to preserve utility (e.g., 14.65% RVQA), validating the advantage of selective neuron editing.

## 4.6 Visualization

We visualize activation residuals across layers using heatmaps to assess the forgetting and retention behavior of different unlearning methods. Specifically, we input both forget-set and retain-set samples into the unlearned MLLMs and record activation values at each FFN layer. These are compared with the vanilla model’s activations, and absolute residuals are used to generate the heatmaps. Darker colors indicate greater deviation from the original model (stronger forgetting), while lighter colors reflect better retention. Experiments are conducted on Qwen2.5-VL using MLLMU-

Bench (5% forget ratio) across generation tasks. Results for generation are shown in Fig. 6. As shown in Fig. 6(a) and Fig. 6(c), baseline methods yield consistently shallow color intensities, especially under textual inputs, suggesting limited forgetting. Moreover, similar intensities across forget and retain sets indicate poor separation of specific and general knowledge. In contrast, MIP-Editor exhibits clear modality-aware behavior: deeper residuals on the forget-set and lighter residuals on the retain-set, particularly under textual inputs, demonstrating effective cross-modal unlearning with minimal performance degradation.

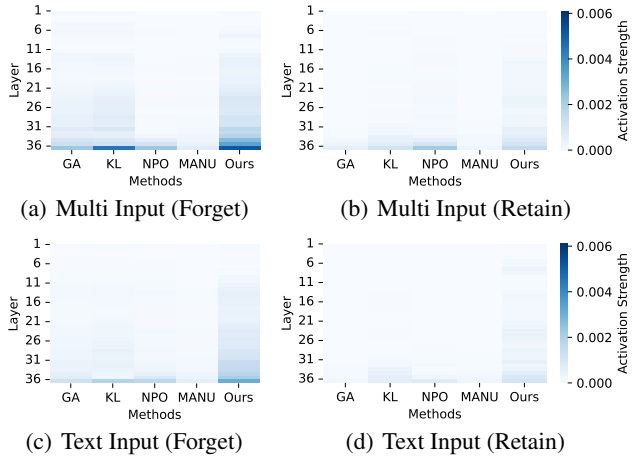


Figure 6: Layer-wise visualization of knowledge retention in the language FFN of MLLMs across forget and retain sets on MLLMU-Bench. GA: Grad\_Diff; Ours: MIP-Editor.

## 4.7 Specific Information Separability

To assess the effectiveness of unlearning methods in separating specific information from general knowledge in MLLMs, we train an MLP-based binary classifier using the output logits of the post-unlearning model. Experiments on MLLMU-Bench and CLEAR with Qwen2.5-VL evaluate two settings: (1) classification over the full fine-tuning set and (2) classification on CLEAR’s generation tasks (Multi and Text). As shown in Fig. 7, MIP-Editor consistently achieves the highest classification accuracy, exceeding 85% across datasets and input types, indicating clearer behavioral separation between specific and general inputs. In contrast, GA, KL, NPO, and MANU perform near random (around 50%) on MLLMU-Bench, showing limited separation capability. On CLEAR’s text generation tasks, where questions and answers lack visual modality, the performance of the classification becomes harder to distinguish. Nonetheless, MIP-Editor still outperforms all baselines.

## 5 Related Works

**Fine-tuning for MLLM Unlearning** Recent efforts in MU aim to remove specific knowledge from models for privacy and safety. Early approaches primarily focus on LLMs and employ gradient ascent (Thudi et al. 2022; Liu, Liu, and Stone 2022), KL minimization (Nguyen, Low, and Jaillet

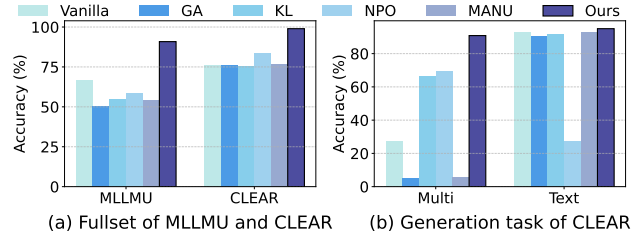


Figure 7: Classification of specific vs. general data using Qwen2.5-VL, including (a) full-set classification on MLLMU-Bench and CLEAR, and (b) generation-task classification on CLEAR (Multi and Text).

2020), and preference-based objectives such as NPO (Zhang et al. 2024), with applications in toxicity mitigation (Chen et al. 2025) and hallucination reduction (Xing et al. 2024). However, these methods are limited to the textual modality. Multimodal unlearning for MLLMs remains underexplored. To facilitate research, dedicated benchmarks such as MLLMU-BENCH (Liu et al. 2025a) and CLEAR (Dontsov et al. 2024) have been introduced. Recent studies (Yang et al. 2024; Cheng and Amiri 2024; Li et al. 2024b; Huo et al. 2025) attempt to erase visual concepts via fine-tuning. Nonetheless, these methods require full-model fine-tuning and ignore the modular design of MLLMs.

**Neuron Editing in Large Language Models** Neuron-editing has gained attention as a means to modify LLM behavior in targeted domains while preserving general performance. Recent studies have examined how Pretrained Language Models store knowledge (Chen et al. 2024; Li et al. 2023; Cao et al. 2024; Lamparth and Reuel 2024), enabling controlled neuron-level interventions. Prior work has applied neuron editing to machine unlearning (Wu, Hashemi, and Srinivasa 2022; Hase et al. 2023; Gandikota et al. 2023), harmful output mitigation (Hu et al. 2024), continual learning (Biesialska, Biesialska, and Ruiz Costa-Jussà 2020), and privacy preservation (Wu et al. 2023). In multimodal settings, MANU (Liu et al. 2025b) proposes neuron-level editing for modality-specific forgetting. However, its scoring strategy lacks alignment with textual forgetting dynamics, and its zero-out pruning may disrupt critical reasoning paths. Our approach addresses these limitations via path-aware editing that targets coherent, modality-specific neuron sequences for more effective unlearning.

## 6 Conclusion

In this paper, we address machine unlearning in Multimodal Large Language Models (MLLMs), highlighting key limitations of existing methods, such as cross-modal inconsistency and general performance degradation. To tackle these issues, we propose MIP-Editor, a multimodal pathway-editor that identifies influential neuron paths in each modality and applies path-aware editing through representation misdirection. Experiments demonstrate that MIP-Editor achieves effective unlearning of forgetting knowledge while preserving general utility. This work offers a principled framework for fine-grained knowledge removal in MLLMs.

## Acknowledgements

This work was supported in part by Hong Kong RGC Theme-based Research Scheme (TRS) under Grant T43-513/23-N, in part by the NSFC and Hong Kong RGC Collaborative Research Scheme under Grant 62321166652, in part by the Guangdong Basic and Applied Basic Research Foundation under Grant 2025A1515011996, and in part by the Fundamental Research Funds for the Central University under Grant CXTD202406. We also thank the grant from NVIDIA and utilized NVIDIA A100 GPUs through the NVIDIA Academic Grants Program.

## References

Biesialska, M. M.; Biesialska, K.; and Ruiz Costa-Jussà, M. 2020. Continual lifelong learning in natural language processing: a survey. In *COLING 2020, The 28th International Conference on Computational Linguistics: December 8-13, 2020, Barcelona, Spain (online): proceedings of the conference*, 6523–6541. Association for Computational Linguistics.

Caffagni, D.; Cocchi, F.; Barsellotti, L.; Moratelli, N.; Sarto, S.; Baraldi, L.; Cornia, M.; and Cucchiara, R. 2024. The Revolution of Multimodal Large Language Models: A Survey. In *Findings of the Association for Computational Linguistics ACL 2024*, 13590–13618.

Cao, B.; Tang, Q.; Lin, H.; Jiang, S.; Dong, B.; Han, X.; Chen, J.; Wang, T.; and Sun, L. 2024. Retentive or Forgetful? Diving into the Knowledge Memorizing Mechanism of Language Models. In *Proceedings of the 2024 Joint International Conference on Computational Linguistics, Language Resources and Evaluation (LREC-COLING 2024)*, 14016–14036.

Chen, J.; Deng, Z.; Zheng, K.; Yan, Y.; Liu, S.; Wu, P.; Jiang, P.; Liu, J.; and Hu, X. 2025. SAFERASER: Enhancing Safety in Multimodal Large Language Models through Multimodal Machine Unlearning. *arXiv preprint arXiv:2502.12520*.

Chen, Y.; Cao, P.; Chen, Y.; Liu, K.; and Zhao, J. 2024. Journey to the center of the knowledge neurons: Discoveries of language-independent knowledge neurons and degenerate knowledge neurons. In *Proceedings of the AAAI Conference on Artificial Intelligence*, volume 38, 17817–17825.

Cheng, J.; and Amiri, H. 2024. Multidelete for multimodal machine unlearning. In *European Conference on Computer Vision*, 165–184. Springer.

Chundawat, V. S.; Tarun, A. K.; Mandal, M.; and Kankanhalli, M. 2023. Zero-shot machine unlearning. *IEEE Transactions on Information Forensics and Security*, 18: 2345–2354.

Dai, D.; Dong, L.; Hao, Y.; Sui, Z.; Chang, B.; and Wei, F. 2022. Knowledge Neurons in Pretrained Transformers. In *Proceedings of the 60th Annual Meeting of the Association for Computational Linguistics (Volume 1: Long Papers)*, 8493–8502.

Dang, H.-T.; Pham, T.; Thanh-Tung, H.; and Inoue, N. 2025. On Effects of Steering Latent Representation for Large Language Model Unlearning. In *Proceedings of the AAAI Conference on Artificial Intelligence*, volume 39, 23733–23742.

Dontsov, A.; Korzh, D.; Zhavoronkin, A.; Mikheev, B.; Bobkov, D.; Alanov, A.; Rogov, O. Y.; Oseledets, I.; and Tuttubalina, E. 2024. Clear: Character unlearning in textual and visual modalities. *arXiv preprint arXiv:2410.18057*.

Fan, C.; Liu, J.; Lin, L.; Jia, J.; Zhang, R.; Mei, S.; and Liu, S. 2024. Simplicity Prevails: Rethinking Negative Preference Optimization for LLM Unlearning. In *Neurips Safe Generative AI Workshop 2024*.

Gandikota, R.; Materzynska, J.; Fiotto-Kaufman, J.; and Bau, D. 2023. Erasing concepts from diffusion models. In *Proceedings of the IEEE/CVF International Conference on Computer Vision*, 2426–2436.

Hase, P.; Bansal, M.; Kim, B.; and Ghandeharioun, A. 2023. Does localization inform editing? surprising differences in causality-based localization vs. knowledge editing in language models. *Advances in Neural Information Processing Systems*, 36: 17643–17668.

Hu, E. J.; Wallis, P.; Allen-Zhu, Z.; Li, Y.; Wang, S.; Wang, L.; Chen, W.; et al. 2022. LoRA: Low-Rank Adaptation of Large Language Models. In *International Conference on Learning Representations*.

Hu, X.; Li, D.; Hu, B.; Zheng, Z.; Liu, Z.; and Zhang, M. 2024. Separate the wheat from the chaff: Model deficiency unlearning via parameter-efficient module operation. In *Proceedings of the AAAI Conference on Artificial Intelligence*, volume 38, 18252–18260.

Huo, J.; Yan, Y.; Zheng, X.; Lyu, Y.; Zou, X.; Wei, Z.; and Hu, X. 2025. MMUNLEARNER: Reformulating Multimodal Machine Unlearning in the Era of Multimodal Large Language Models.

Jia, J.; Liu, J.; Ram, P.; Yao, Y.; Liu, G.; Liu, Y.; Sharma, P.; and Liu, S. 2023. Model sparsity can simplify machine unlearning. *Advances in Neural Information Processing Systems*, 36: 51584–51605.

Lamparth, M.; and Reuel, A. 2024. Analyzing and editing inner mechanisms of backdoored language models. In *Proceedings of the 2024 ACM Conference on Fairness, Accountability, and Transparency*, 2362–2373.

Li, H.; Deng, G.; Liu, Y.; Wang, K.; Li, Y.; Zhang, T.; Liu, Y.; Xu, G.; Xu, G.; and Wang, H. 2024a. Digger: Detecting Copyright Content Mis-usage in Large Language Model Training. *CoRR*.

Li, J.; Wei, Q.; Zhang, C.; Qi, G.; Du, M.; Chen, Y.; Bi, S.; and Liu, F. 2024b. Single image unlearning: Efficient machine unlearning in multimodal large language models. *Advances in Neural Information Processing Systems*, 37: 35414–35453.

Li, N.; Pan, A.; Gopal, A.; Yue, S.; Berrios, D.; Gatti, A.; Li, J. D.; Dombrowski, A.-K.; Goel, S.; Mukobi, G.; et al. 2024c. The WMDP benchmark: measuring and reducing malicious use with unlearning. In *Proceedings of the 41st International Conference on Machine Learning*, 28525–28550.

Li, Z.; Zhang, N.; Yao, Y.; Wang, M.; Chen, X.; and Chen, H. 2023. Unveiling the Pitfalls of Knowledge Editing for Large Language Models. *Corr*.

Liu, B.; Liu, Q.; and Stone, P. 2022. Continual learning and private unlearning. In *Conference on Lifelong Learning Agents*, 243–254. PMLR.

Liu, H.; Li, C.; Wu, Q.; and Lee, Y. J. 2023. Visual instruction tuning. *Advances in neural information processing systems*, 36: 34892–34916.

Liu, Z.; Dou, G.; Jia, M.; Tan, Z.; Zeng, Q.; Yuan, Y.; and Jiang, M. 2025a. Protecting Privacy in Multimodal Large Language Models with MLLMU-Bench. In *Proceedings of the 2025 Conference of the Nations of the Americas Chapter of the Association for Computational Linguistics: Human Language Technologies (Volume 1: Long Papers)*, 4105–4135.

Liu, Z.; Dou, G.; Yuan, X.; Zhang, C.; Tan, Z.; and Jiang, M. 2025b. Modality-Aware Neuron Pruning for Unlearning in Multimodal Large Language Models. *Proceedings of the 63nd Annual Meeting of the Association for Computational Linguistics*.

Lu, K.; Wang, Z.; Mardziel, P.; and Datta, A. 2021. Influence patterns for explaining information flow in bert. *Advances in Neural Information Processing Systems*, 34: 4461–4474.

Łucki, J.; Wei, B.; Huang, Y.; Henderson, P.; Tramèr, F.; and Rando, J. 2025. An Adversarial Perspective on Machine Unlearning for AI Safety. *Transactions on Machine Learning Research*.

Maini, P.; Feng, Z.; Schwarzschild, A.; Lipton, Z. C.; and Kolter, J. Z. 2024. TOFU: A Task of Fictitious Unlearning for LLMs.

Nguyen, Q. P.; Low, B. K. H.; and Jaillet, P. 2020. Variational bayesian unlearning. *Advances in Neural Information Processing Systems*, 33: 16025–16036.

Pan, H.; Cao, Y.; Wang, X.; Yang, X.; and Wang, M. 2024. Finding and Editing Multi-Modal Neurons in Pre-Trained Transformers. In *Findings of the Association for Computational Linguistics ACL 2024*, 1012–1037. Association for Computational Linguistics.

Paszke, A.; Gross, S.; Massa, F.; Lerer, A.; Bradbury, J.; Chanan, G.; Killeen, T.; Lin, Z.; Gimelshein, N.; Antiga, L.; et al. 2019. Pytorch: An imperative style, high-performance deep learning library. *Advances in neural information processing systems*, 32.

Pi, R.; Han, T.; Zhang, J.; Xie, Y.; Pan, R.; Lian, Q.; Dong, H.; Zhang, J.; and Zhang, T. 2024. MLLM-Protector: Ensuring MLLM’s Safety without Hurting Performance. In *Proceedings of the 2024 Conference on Empirical Methods in Natural Language Processing*, 16012–16027.

Radford, A.; Kim, J. W.; Hallacy, C.; Ramesh, A.; Goh, G.; Agarwal, S.; Sastry, G.; Askell, A.; Mishkin, P.; Clark, J.; et al. 2021. Learning transferable visual models from natural language supervision. In *International conference on machine learning*, 8748–8763. PMLR.

Sato, Y.; and Takagi, T. 2025. Identifying Multi-modal Knowledge Neurons in Pretrained Transformers via Two-stage Filtering. *arXiv preprint arXiv:2503.22941*.

Si, N.; Zhang, H.; Chang, H.; Zhang, W.; Qu, D.; and Zhang, W. 2023. Knowledge unlearning for llms: Tasks, methods, and challenges. *arXiv preprint arXiv:2311.15766*.

Thudi, A.; Deza, G.; Chandrasekaran, V.; and Papernot, N. 2022. Unrolling sgd: Understanding factors influencing machine unlearning. In *2022 IEEE 7th European Symposium on Security and Privacy (EuroS&P)*, 303–319. IEEE.

Wang, P.; Bai, S.; Tan, S.; Wang, S.; Fan, Z.; Bai, J.; Chen, K.; Liu, X.; Wang, J.; Ge, W.; et al. 2024. Qwen2-vl: Enhancing vision-language model’s perception of the world at any resolution. *arXiv preprint arXiv:2409.12191*.

Wang, Y.; Liu, Y.; Shi, Y.; Li, C.; Pang, A.; Yang, S.; Yu, J.; and Ren, K. 2025. Discovering Influential Neuron Path in Vision Transformers. In *The Thirteenth International Conference on Learning Representations*.

Wolf, T.; Debut, L.; Sanh, V.; Chaumond, J.; Delangue, C.; Moi, A.; Cistac, P.; Rault, T.; Louf, R.; Funtowicz, M.; Davison, J.; Shleifer, S.; von Platen, P.; Ma, C.; Jernite, Y.; Plu, J.; Xu, C.; Scao, T. L.; Gugger, S.; Drame, M.; Lhoest, Q.; and Rush, A. M. 2020. Transformers: State-of-the-Art Natural Language Processing. In *Proceedings of the 2020 Conference on Empirical Methods in Natural Language Processing: System Demonstrations*, 38–45. Association for Computational Linguistics.

Wu, G.; Hashemi, M.; and Srinivasa, C. 2022. Puma: Performance unchanged model augmentation for training data removal. In *Proceedings of the AAAI conference on artificial intelligence*, volume 36, 8675–8682.

Wu, X.; Li, J.; Xu, M.; Dong, W.; Wu, S.; Bian, C.; and Xiong, D. 2023. DEPN: Detecting and Editing Privacy Neurons in Pretrained Language Models. In *Proceedings of the 2023 Conference on Empirical Methods in Natural Language Processing*, 2875–2886.

Xing, S.; Zhao, F.; Wu, Z.; An, T.; Chen, W.; Li, C.; Zhang, J.; and Dai, X. 2024. EFUF: Efficient Fine-Grained Unlearning Framework for Mitigating Hallucinations in Multimodal Large Language Models. In *Proceedings of the 2024 Conference on Empirical Methods in Natural Language Processing*, 1167–1181.

Yang, T.; Dai, L.; Liu, Z.; Wang, X.; Jiang, M.; Tian, Y.; and Zhang, X. 2024. CLIPERase: Efficient Unlearning of Visual-Textual Associations in CLIP. *arXiv preprint arXiv:2410.23330*.

Yao, Y.; Wang, P.; Tian, B.; Cheng, S.; Li, Z.; Deng, S.; Chen, H.; and Zhang, N. 2023. Editing Large Language Models: Problems, Methods, and Opportunities. In *The 2023 Conference on Empirical Methods in Natural Language Processing*.

Zhang, R.; Lin, L.; Bai, Y.; and Mei, S. 2024. Negative Preference Optimization: From Catastrophic Collapse to Effective Unlearning. In *First Conference on Language Modeling*.

Zhang, S.; Dong, L.; Li, X.; Zhang, S.; Sun, X.; Wang, S.; Li, J.; Hu, R.; Zhang, T.; Wu, F.; et al. 2023. Instruction tuning for large language models: A survey. *arXiv preprint arXiv:2308.10792*.

## A1 Supplemental Materials of MIP-Editor

### A1.1 Overall process of MIP-Editor.

We present the overall workflow of MIP-Editor in the form of pseudocode, including both the inter-layer integration-based identification of influential neuron paths and the complete unlearning procedure.

---

Algorithm 2: Framework of MIP-Editor

---

**Input:** MLLM  $M_\theta$  with  $L^t$  textual layers and  $L^v$  visual layers; forget-set  $D^f = \{(I_j^f, T_j^f)\}_{j=1}^{N_f}$ ; retain set  $D^r = \{(I_j^r, T_j^r)\}_{j=1}^{N_r}$   
**Output:** Unlearned MLLM  $M_{\theta^*}$

- 1: // Stage 1: Locating Influential Neuron Paths
- 2:  $\mathcal{P}^t, \mathcal{P}^v \leftarrow$  Algorithm 1( $M_\theta, (I, T)$ )
- 3: // Stage 2: Pruning Non-Path Neurons
- 4: **for** each textual layer  $l \in [1, L^t]$  **do**
- 5:   Set  $\tilde{w}_j^l \leftarrow 0, \forall j \in \mathcal{P}^t[l]$
- 6: **end for**
- 7: **for** each visual layer  $l \in [1, L^v]$  **do**
- 8:   Set  $\tilde{z}_j^l \leftarrow 0, \forall j \in \mathcal{P}^v[l]$
- 9: **end for**
- 10: // Stage 3: Editing with RMisU on Pruned Paths
- 11: Sample random unit vector  $\mathbf{u} \sim \text{Uniform}(\mathbb{S}^{d-1})$
- 12: **for** each training step **do**
- 13:   **for** each  $x^f \in D^f$  **do**
- 14:     Compute target vector  $\mathbf{v}^f$  by  $\mathbf{u}$  (Eq. 13)
- 15:     Compute forgetting loss  $\mathcal{L}_{\text{RMisU}}^f$  (Eq. 14)
- 16:   **end for**
- 17:   **for** each  $x^r \in D^r$  **do**
- 18:     Compute retention loss  $\mathcal{L}_{\text{RMisU}}^r$  (Eq. 15)
- 19:   **end for**
- 20:   Update  $\theta^*$  on  $\mathcal{P}^t \cup \mathcal{P}^v$  using gradient descent on total loss:  $\mathcal{L}_{\text{adaptive}} = \mathcal{L}_{\text{RMisU}}^f + \gamma \cdot \mathcal{L}_{\text{RMisU}}^r$
- 21: **end for**
- 22: **return**  $M_{\theta^*}$

---

### A1.2 Complexity Analysis

We analyze the time and space complexity of MIP-Editor when applied to a single input sample. The overall procedure consists of two stages: locating influential paths and editing with RMisU.

**Time Complexity** In the first stage, path locating is conducted independently for the text and vision branches. For the text branch, we consider  $L^t$  transformer layers. At each layer  $l$ , all candidate neurons  $|w_l^t|$  are evaluated using the discretized Inter-layer Gradient Integration (Eq. 4). This process requires  $m$  Riemann approximation points per neuron, where each point involves a forward and backward pass. Furthermore, gradient accumulation across all previous layers is performed for every candidate neuron. As a result, the overall time complexity for the text branch is:

$$O \left( C_{\text{grad}} \cdot m \cdot L^t \cdot \sum_{l=1}^{L^t} |w_l^t| \right), \quad (\text{A1})$$

where  $C_{\text{grad}}$  denotes the cost of one forward-backward pass.

The vision branch follows an analogous computation. For each of the  $L^v$  vision layers, we apply the Inter-layer Fisher Integration (Eq. 6) to every candidate neuron  $|z_l^v|$ , also using  $m$  integration points. This yields a time complexity of:

$$O \left( C_{\text{grad}} \cdot m \cdot L^v \cdot \sum_{l=1}^{L^v} |z_l^v| \right), \quad (\text{A2})$$

In the second stage, editing with RMisU is applied only to the selected neurons along the influential paths. The training objective includes both retention and forgetting losses, together with a representation misalignment penalty. Since the number of updated parameters is linear in  $L^t + L^v$ , the cost of this stage is relatively small and denoted as  $O(C_{\text{ft}})$ . Therefore, the total

time complexity for processing a single sample is:

$$O \left( C_{\text{grad}} \cdot m \cdot \left( L^t \cdot \sum_{l=1}^{L^t} |w_l^t| + L^v \cdot \sum_{l=1}^{L^v} |z_l^v| \right) + C_{\text{ft}} \right). \quad (\text{A3})$$

**Space Complexity** The space complexity is primarily dictated by the need to store intermediate activations and gradients during the integration phase. For each of the  $m$  interpolation steps, we cache the activations and gradients of all candidate neurons, leading to a memory cost of  $O \left( m \cdot \sum_{l=1}^{L^t} |w_l^t| + m \cdot \sum_{l=1}^{L^v} |z_l^v| \right)$ . Additionally, in the RMisU phase, we maintain optimizer states (e.g., momentum or adaptive moments) for only the selected neurons, resulting in an additional cost of  $O(L^t + L^v)$ . The total space complexity is thus given by:

$$O \left( m \cdot \left( \sum_{l=1}^{L^t} |w_l^t| + \sum_{l=1}^{L^v} |z_l^v| \right) + L^t + L^v \right). \quad (\text{A4})$$

## A2 Supplemental Experiments

### A2.1 Datasets Details

**MLLMU-Bench** is a benchmark specifically designed to facilitate research in multimodal machine unlearning. It comprises 500 fictitious user profiles and 153 public celebrity profiles, each associated with over 14 personalized question–answer pairs spanning both multimodal and textual modalities. In this paper, we partition MLLMU-Bench into six distinct subsets to comprehensively evaluate the effectiveness, generalizability, and utility of various unlearning methods, particularly in terms of their handling of visual and textual knowledge. Compared with CLEAR, MLLMU-Bench yields more stable and consistent performance across different experimental configurations. This stability makes it a more reliable basis for comparative analysis. Therefore, we conduct most of our ablation and component studies using MLLMU-Bench.

**CLEAR** is another open-source benchmark developed to assess unlearning performance in multimodal settings. It contains 200 synthetic author profiles, accompanied by 3,770 visual question–answer pairs and 4,000 textual ones. CLEAR builds upon the TOFU benchmark (Maini et al. 2024) by introducing portrait images corresponding to each entity referenced in the question–answer pairs. In our experimental practice, as well as in alignment with observations reported by MMUnlearner (Huo et al. 2025), we find that even minor adjustments to learning rate or batch size on CLEAR often result in complete model collapse. Such instability manifests as a drastic drop in both classification and generation accuracy, consistent with the performance degradation reported in the original CLEAR benchmark. Therefore, we treat the results on CLEAR as supplementary evidence.

### A2.2 Detailed Baselines

We set the following strong baselines in the machine unlearning for MLLMs.

**GA\_Diff** The Gradient Ascent (GA) approach suppresses forgetting-related knowledge by performing inverse gradient updates on the forget-set  $D^f$ . GA\_Diff extends this method by simultaneously applying opposing gradients to  $D^f$  and standard gradient descent updates to the retain set  $D^r$ , thereby promoting unlearning while preserving generalization. The combined loss function is defined as:

$$\mathcal{L}_{\text{GA\_Diff}} = L(D^f, \theta) - L(D^r, \theta), \quad (\text{A5})$$

where  $L$  denotes the negative log-likelihood loss.

**KL\_Min** The KL Minimization approach enforces forgetting by encouraging divergence from the original model’s predictions on  $D^f$ , while simultaneously aligning the unlearned model’s behavior on  $D^r$  with that of the original model. Formally, the per-token KL divergence is defined as:

$$\Phi(x_{<i}) = \text{KL}(P(x_{<i}|\theta) \parallel P(x_{<i}|\theta_0)), \quad (\text{A6})$$

where  $P(\cdot|\theta)$  and  $P(\cdot|\theta_0)$  denote the output distributions of the unlearned and original models, respectively. The KL-based regularization term is:

$$\mathcal{L}_{\text{KL}} = \frac{1}{|D^f|} \sum_{x \in D^f} \frac{1}{|x|} \sum_{i=2}^{|x|} \Phi(x_{<i}). \quad (\text{A7})$$

The overall objective is then given by:

$$\mathcal{L}_{\text{KL\_Min}} = -L(D^f, \theta) + \mathcal{L}_{\text{KL}}. \quad (\text{A8})$$

Table A1: Hyperparameter configurations for training the vanilla model and performing unlearning across different MLLM backbones and datasets.

Dataset		MLLMU-Bench		CLEAR	
MLLM		Qwen2.5-VL-3B-Instruct	LLaVA-1.5-7B	Qwen2.5-VL-3B-Instruct	LLaVA-1.5-7B
Training	Epochs	4	4	4	4
	Batch Size	4	4	4	4
	Optimizer	Adam	Adam	Adam	Adam
	LoRA	TRUE	TRUE	TRUE	TRUE
	Learning Rate	2e-5	2e-5	2e-5	2e-5
Unlearning	Epochs	4	4	4	4
	Batch Size	4	4	4	4
	Optimizer	Adam	Adam	Adam	Adam
	LoRA	TRUE	TRUE	TRUE	TRUE
	Learning Rate	2e-5	2e-5	2e-5	2e-5

**NPO** Negative Preference Optimization (NPO) frames unlearning as a preference optimization task by treating the forget-set  $D^f$  as dispreferred. An oracle model  $\pi_{\text{ref}}$ , trained exclusively on  $D^r$ , serves as a reference to guide the current model  $\pi_\theta$  away from retaining knowledge of  $D^f$ . The NPO objective is defined as:

$$\mathcal{L}_{\text{NPO}} = \frac{2}{\beta} \mathbb{E}_{(x,y) \in D^f} \left[ \log \left( 1 + \left( \frac{\pi_\theta(y|x)}{\pi_{\text{ref}}(y|x)} \right)^\beta \right) \right], \quad (\text{A9})$$

where  $\pi_\theta(y|x)$  is the current model's prediction probability and  $\pi_{\text{ref}}(y|x)$  is the prediction from the reference model. The hyperparameter  $\beta$  controls the sharpness of the preference contrast and is set to 0.4 in our experiments.

**MANU** MANU identifies important multimodal neurons based on point-wise activation statistics and prunes those deemed most influential to the forget-set. For a given neuron  $n$ , its importance is aggregated from a set of scoring functions  $\mathcal{K} = \{\text{abs}, \text{freq}, \text{var}, \text{rms}\}$ :

$$\mathcal{I}(D, n) = \sum_{k \in \mathcal{K}} I_k(D, n). \quad (\text{A10})$$

The relative importance score is then defined as:

$$S_n = \frac{\mathcal{I}(D^f, n)}{\mathcal{I}(D^r, n) + \epsilon}. \quad (\text{A11})$$

The top- $\alpha\%$  neurons with the highest  $S_n$  values are selected and pruned:

$$\mathcal{N} = \{n \mid S_n \text{ is among the top } \alpha\%\}. \quad (\text{A12})$$

For each  $n \in \mathcal{N}$ , the neuron is pruned by setting its associated weights to zero.

### A2.3 Implementation Details

To evaluate the generalizability of MU methods across model scales, we employ Qwen2.5-3B-Instruct and LLaVA-1.5-7B as base models. Qwen2.5-3B-Instruct excels at instruction following, while the larger LLaVA-1.5-7B, with its greater parameter capacity, captures finer multimodal patterns. For reproducibility, the experimental configurations for all unlearning methods are summarized in Table A1, based on the official setups of MLLMU-BENCH and CLEAR, Pytorch (Paszke et al. 2019) and Transformers (Wolf et al. 2020) are used to construct experimental environments. LoRA (Hu et al. 2022) is applied to enable efficient adaptation. All experiments were accelerated on the NVIDIA A100 GPU.

### A2.4 Additional Influential Path v.s. Influential Neurons

We provide additional comparison between the influential path and neurons, the results of the classification task are shown in Fig. A1.

### A2.5 Additional Visualizations

We provide additional visualization results of the distribution of activation residuals across layers for the classification task in Fig. A2.

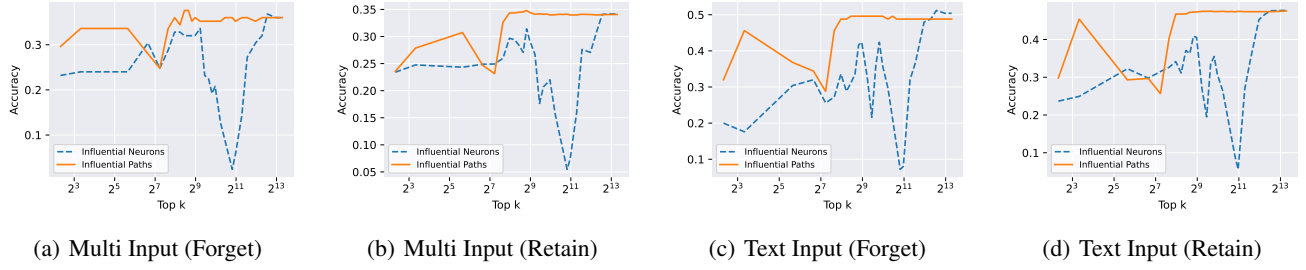


Figure A1: Performance comparison on classification tasks between influential neuron paths and point-wise influential neurons under varying top- $k$  neuron selections.

Table A2: Additional performances of baseline methods and MIP-Editor on machine unlearning tasks. F: Forget-set; R:Retain-set; VQA:Vision Question Answer; QA: Question Answer; VGEN: Vision Generation; GEN: Generation.

Method		MLLMU-Bench with 10% forget ratio						CLEAR with 10% forget ratio					
Task	Metric	FVQA	RVQA	FVGEN	RVGEN	FQA	RQA	FVQA	RVQA	FVGEN	RVGEN	FGEN	RGEN
Qwen2.5-VL-3B-Instruct													
Vanilla		37.20%	37.91%	0.4526	0.4336	54.80%	46.59%	78.31%	77.47%	0.3199	0.2964	0.3911	0.3895
GA.Diff		30.00%	32.96%	0.4042	0.4472	20.40%	22.80%	4.76%	5.06%	0.2613	0.2498	0.3794	0.3865
KL_Min		21.60%	26.10%	0.1834	0.1872	44.00%	41.83%	3.70%	8.35%	0.3221	0.3155	0.3221	0.3155
NPO		35.20%	36.44%	0.3987	0.3839	54.40%	45.96%	8.20%	10.89%	0.1233	0.1165	0.1233	0.1165
MANU		32.80%	34.48%	0.4242	0.4472	48.40%	43.38%	78.31%	77.22%	0.3899	0.3890	0.3899	0.3890
MIP-Editor		5.20%	45.26%	0.935	0.4316	36.40%	46.15%	4.50%	31.39%	0.0785	0.1473	0.3683	0.3705
Llava-1.5-7B													
Vanilla		52.80%	51.67%	0.4672	0.4986	52.40%	52.34%	44.71%	43.03%	0.3084	0.2915	0.3514	0.3544
GA.Diff		43.60%	44.80%	0.3524	0.3822	45.60%	46.09%	20.11%	18.23%	0.2462	0.2334	0.0666	0.0203
KL_Min		30.80%	33.27%	0.3816	0.3747	37.20%	36.17%	11.64%	12.66%	0.2793	0.0806	0.2648	0.0843
NPO		48.40%	46.77%	0.4669	0.4982	52.00%	50.65%	10.58%	12.15%	0.1623	0.1446	0.0245	0.0206
MANU		53.20%	52.16%	0.4743	0.4997	51.60%	52.34%	44.97%	43.29%	0.3042	0.2898	0.3496	0.3524
MIP-Editor		32.00%	41.07%	0.3443	0.3932	33.20%	38.53%	8.47%	49.87%	0.1393	0.1603	0.1477	0.2584
Method		MLLMU-Bench with 15% forget ratio						CLEAR with 1% forget ratio					
Task	Metric	FVQA	RVQA	FVGEN	RVGEN	FQA	RQA	FVQA	RVQA	FVGEN	RVGEN	FGEN	RGEN
Qwen2.5-VL-3B-Instruct													
Vanilla		38.67%	37.50%	0.4357	0.4358	49.87%	46.98%	60.00%	77.47%	0.3094	0.3012	0.4008	0.3893
GA.Diff		34.67%	33.68%	0.4192	0.4468	18.40%	22.26%	57.14%	87.09%	0.3314	0.3526	0.3909	0.3909
KL_Min		33.33%	28.44%	0.3234	0.3322	46.67%	42.12%	48.57%	65.82%	0.2281	0.2236	0.2686	0.2734
NPO		38.13%	36.13%	0.3757	0.3938	48.80%	46.16%	54.29%	72.66%	0.3500	0.4114	0.1458	0.1001
MANU		35.73%	34.95%	0.4203	0.4386	41.60%	45.13%	54.29%	76.71%	0.2977	0.3001	0.4186	0.3912
MIP-Editor		6.67%	55.66%	0.1653	0.3888	33.06%	46.36%	0.00%	25.82%	0.1354	0.2796	0.1195	0.3796
Llava-1.5-7B													
Vanilla		52.53%	51.51%	0.4783	0.4990	48.80%	53.11%	65.71%	43.54%	0.3164	0.2930	0.3629	0.3541
GA.Diff		52.80%	51.37%	0.3529	0.3587	48.00%	45.52%	14.29%	18.73%	0.3160	0.3068	0.3718	0.3598
KL_Min		9.07%	8.54%	0.2346	0.2442	33.07%	28.73%	2.86%	24.81%	0.2552	0.2376	0.2110	0.2927
NPO		50.33%	47.31%	0.4690	0.4959	47.20%	50.94%	17.14%	15.44%	0.1708	0.1595	0.0339	0.4000
MANU		52.80%	51.37%	0.4776	0.5003	47.73%	52.31%	68.57%	43.29%	0.3040	0.2929	0.3603	0.3534
MIP-Editor		33.33%	39.91%	0.3463	0.4074	34.40%	38.63%	20.00%	42.03%	0.1373	0.1729	0.0889	0.1601

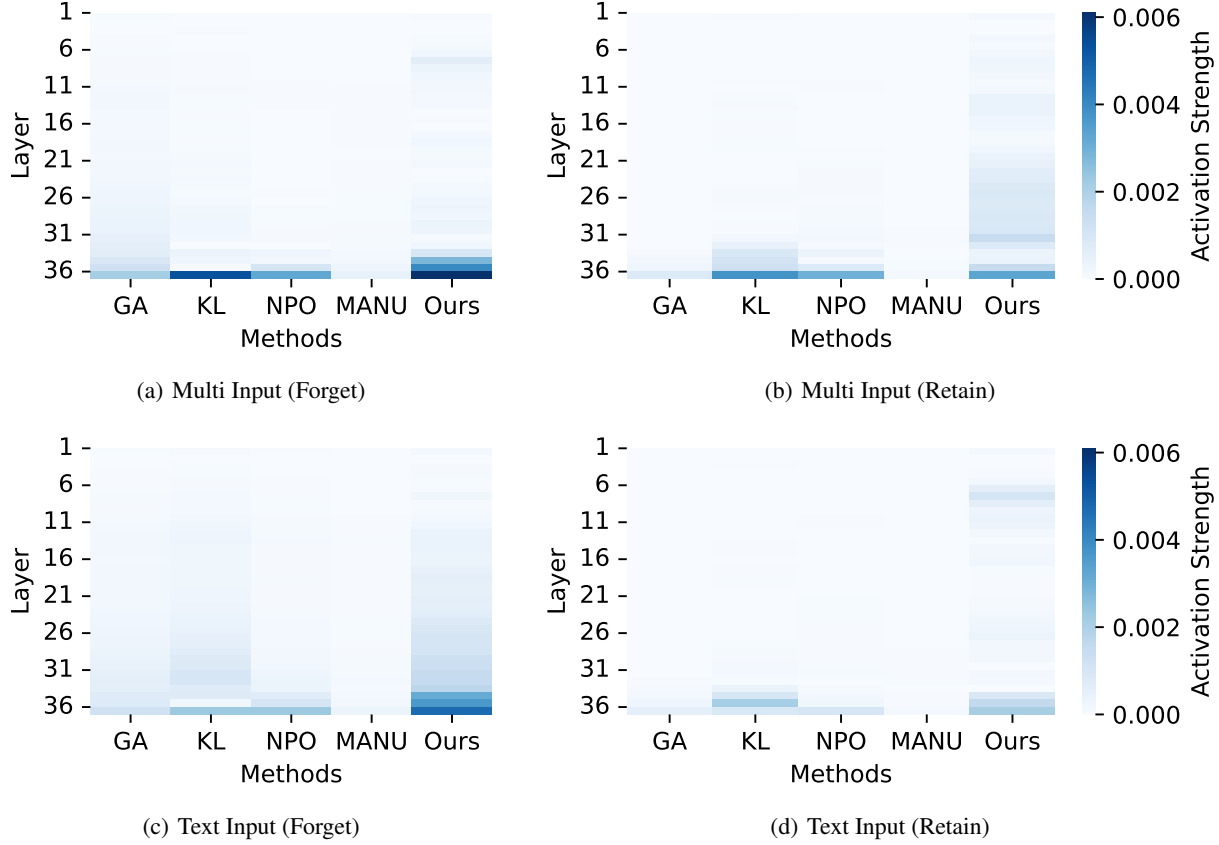


Figure A2: Layer-wise visualization of knowledge retention in the language FFN of MLLMs across forget and retain sets on MLLMU-Bench. GA: Grad\_Diff; Ours: MIP-Editor.

## A2.6 Additional Unlearning Performances

This section reports the unlearning performance of MIP-Editor compared with other baselines on MLLMU-Bench at 10% and 15% forget ratios, and on CLEAR at 1% and 10%. Detailed results are presented in Table A2.

## A2.7 Case Study

To further evaluate the effectiveness of unlearning methods, we present qualitative case studies from MLLMU-Bench and CLEAR using the Qwen2.5-VL (Fig. A3). The selected examples include both forget-set and retain-set samples across question answering and image captioning tasks.

For forget-set instances, baseline methods (GA.Diff, KL.Min, NPO, MANU) often generate responses that retain partial or complete semantic overlap with the ground truth, indicating insufficient forgetting. For example, when asked “*What is this person’s primary activity in the image?*”, most baselines still return variations of “attending school.” In contrast, MIP-Editor responds with a semantically unrelated answer, such as “painting in her free time,” effectively disassociating from the forgetting content. Similarly, for the question “*Which university did this person attend?*”, only MIP-Editor correctly outputs “the University of Melbourne,” while others either hallucinate unrelated institutions or avoid the question entirely—demonstrating MIP-Editor’s ability to isolate forget-set knowledge without disrupting adjacent semantics.

On retain-set examples, MIP-Editor better preserves factual accuracy and stylistic fidelity than competing baselines. For instance, in image description tasks, baseline outputs often suffer from minor omissions or inconsistencies, while MIP-Editor maintains coherence even when surface entities are adjusted—highlighting the benefits of path-specific editing for general knowledge retention.

Notably, we observe that GA.Diff and NPO degrade overall language fluency post-unlearning. This stems from their underlying optimization strategies: GA.Diff applies adversarial gradients to  $D^f$ , potentially distorting parameters essential for language modeling; NPO suppresses model confidence on  $D^f$ , which can generalize to similar inputs and destabilize text generation.

Figure A3: Case study of unlearning performance by MIP-Editor and other baselines on various datasets using Qwen2.5-VL.